

Intensification of Sonophotocatalytic Degradation of Ponceau S using Fe - Doped and Undoped ZnO Nano Catalyst

V. K. Mahajan¹, S. G. Shelar², S. P. Patil³, G. H. Sonawane^{1*}

¹Department of Chemistry, Kisan Arts, Commerce and Science College, Parola, Dist- Jalgaon- 425111 (M.S) India

²Department of Chemistry, S.R.N.D Arts, Commerce and Science College, Bhadgaon, Dist.- Jalgaon- 424105 (M.S.) India

³Nano-Chemistry Research Laboratory, N. T. V. S's G. T. Patil Arts, Commerce and Science College, Nandurbar- 425412 (M.S.) India

Received 5 April 2023, accepted in final revised form 24 October 2023

Abstract

Fe-doped ZnO nano catalyst was synthesized by co-precipitation method. The intrinsic characteristics of a prepared nano Fe-doped ZnO catalyst were studied using a variety of techniques including powder X-ray diffraction (XRD), scanning electron microscope (SEM), electron dispersive X-ray spectroscopy (EDS). In this study, degradation of Ponceau S as a dye pollutant was investigated in the presence of ZnO and Fe-doped ZnO nano catalyst using sonolysis, photocatalysis, sonocatalysis and sonophotocatalysis. The UV light and ultrasonic probsonicator at 20 kHz and 150 W powers were used as an irradiation source. The effect of H₂O₂ on sonocatalytic, photocatalytic and sonophotocatalytic degradation was investigated. At optimum conditions the dye degradation efficiency was influenced by addition of H₂O₂, the highest dye degradation was obtained as 98 % by US+UV+Fe-doped ZnO+H₂O₂ for 40 mg/L dye concentration after 90min. The experimental kinetic data followed the pseudo-first order model in doped and undoped sonocatalytic, photocatalytic and sonophotocatalytic processes but the rate constant of sonophotocatalysis is higher than sonocatalysis and photocatalysis process. The sonophotocatalysis was always faster than the respective individual processes due to the more formation of reactive radicals as well as the increase of the active surface area of nano catalyst.

Keywords: Ponceau S; ZnO; Fe-doped ZnO; Ultrasound; Sonocatalyst; Photocatalyst; Sonophotocatalyst; Kinetics.

© 2024 JSR Publications. ISSN: 2070-0237 (Print); 2070-0245 (Online). All rights reserved.
doi: <http://dx.doi.org/10.3329/jsr.v16i1.65455> J. Sci. Res. **16** (1), 265-280 (2024)

1. Introduction

Advanced Oxidation Processes (AOP) involving ultraviolet light, fenton reagents, ozone, ultrasound etc. have been tested individually as well as in combination, in the presence and absence of catalysts for the treatment of wastewater containing pesticides, phenols,

* Corresponding author: drgunvantsonawane@gmail.com

chlorophenols, dyes and other pollutants [1-5]. The mechanism in all these cases involves the formation of active $\cdot\text{OH}$ radicals which degradation of organic pollutants.

The traditional methods as phase-transfer method, biological treatment methods hardly degrade the dye with low molecular weight and high-water solubility, and can cause a secondary environmental pollution [6,7]. The past few years, advanced oxidation processes (AOPs) such as fenton, ozonation, photocatalysis, sonocatalysis and sonophotocatalysis etc. are successfully used for the degradation of dyes, but they cannot achieve complete degradation of pollutants with high concentration in actual applications due to technical limitation [8]. All the existing AOPs, ultrasound is a very effective way to degradation of organic dyes in non- or low-transparent dye effluents. The dye degradation is attributed to much more than sonochemical degradation that result from acoustic cavitation. According to the theoretical and experimental investigations, sonochemistry are related to sonoluminescence because all of them originate from the high temperature condition inside the collapsing bubbles [9].

The ultrasonic, sonocatalytic, photocatalytic and sonophotocatalytic degradation of organic pollutants clearly increases in the presence of a semiconductor oxide, which could be related to the synergistic effect of ultrasound and solid semiconductor. For example, the semiconductor powder provides additional nuclei for cavitation bubble formation, and the mass transfer of pollutants between the solution and the semiconductor surface increases under ultrasonic irradiation. The active surface area of the semiconductor also increases due to de-aggregating by ultrasonic irradiation, and the photocatalyst can be excited by ultrasound-induced luminescence with a high wavelength and increased production of hydroxyl radicals ($\cdot\text{OH}$) in the reaction mixture [10]. Among several semiconductor oxides, Zinc oxide (ZnO) is a semiconducting material with excellent structural, chemical and photocatalytic properties because of its chemical stability, high room-temperature luminescence, good transparency, and high electron mobility [11,12]. ZnO and Fe doped ZnO nano catalyst have desired physical, chemical, and optical properties, including high UV absorption potential, a wide band gap (3.37 eV), and high exciting binding energy (60 meV) [13]. However, pure ZnO nano catalyst has some drawbacks, such as photocorrosion and fast recombination of the generated electron hole pairs [14]. Therefore, reduction of the electron-hole recombination rate of the ZnO nanoparticles can be an effective strategy to improve the catalytic activity. In this regard, rare-earth metals (REMs) have been introduced as possible doping agents to modify the optical and catalytic properties of ZnO [15-19].

Generally, the choice of the dopant element depends on its electronegativity and the difference between the dopant ionic radius and zinc ionic radius. Among all metal dopants, iron (Fe) is the best due to its chemical stability and the dimensions of the ionic radii 0.78 Å and 0.64 Å, for Fe^{2+} and Fe^{3+} respectively, close to the ionic radius of Zn^{2+} (0.74 Å). Thus, thanks to its properties, Fe could easily enter into the ZnO lattice without substantially modifying the crystal structure of the host semiconductor [20].

Different methods were employed to synthesize doped ZnO nanoparticles including hydrothermal or solvothermal methods, sol-gel, laser-assisted chemical vapor deposition,

spray pyrolysis microwave-assisted synthesis combustion, and co-precipitation [21]. However, these methods have many drawbacks. For instance, hydrothermal synthesis requires expensive equipment and the final samples show generally large particle size, while the sol-gel method, which is one of more used for the synthesis of photocatalysts, requires long processing time and toxic organic solvents [22]. To overcome these disadvantages, co-precipitation method has been proposed as a novel technique for the preparation of the ZnO and Fe doped ZnO nano catalyst with controlled morphology and narrow size distribution to obtain an improvement in activity performances and at the same time to reduce the quantities of toxic organic and inorganic solvents.

Dopant ion incorporation is expected to reduce the recombination of electron and hole because the dopant induced shallow donor and acceptor states act as an electron or hole trap, which leads to prolonged carrier diffusion length resulting in better sonophotocatalytic activity. Transition metal doped ZnO particles exhibit novel properties while retaining the properties of the host even when the dopant is uniformly dispersed. Therefore, these particles have been employed to improve sonophotocatalytic activities because it is very easy to incorporate transition metals into many of the methods for preparing ZnO and Fe-doped ZnO nano catalyst. In the present study, iron (Fe)-doped ZnO nano catalyst were synthesized by co-precipitation method. The physical and optical properties of the synthesized samples were carefully investigated, and then, the ultrasonic, sonocatalytic, photocatalytic and sonophotocatalytic activity of the pure and Fe-doped ZnO nanoparticles was studied for the degradation of Ponceau S as a model organic pollutant. The effect of different operational parameters of the ultrasonic, sonocatalytic, photocatalytic and sonophotocatalytic process was investigated.

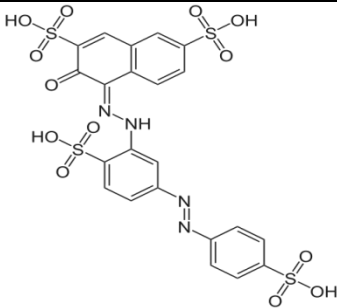
2. Experimental

2.1. Materials and methods

The chemical structure and some characteristics of Ponceau S are given in Table 1. Ponceau S was purchased from Loba Chemie. The pH of the model solution was 8.1. Fe-doped ZnO nano catalyst was synthesized by co-precipitation method. All chemicals used for the synthesis of A.R. grade. The synthesized nano catalyst was characterized by X-Ray diffraction (XRD) (Bruker D8 Advance Diffractometer, Germany), scanning electron microscope (SEM) (Hitachi S-4800, Japan) and electron dispersive X-ray spectroscopy (EDS). The ultrasonic irradiation was produced by using an ultrasonic probsonicator at 20 kHz and 150 W powers (Dakshin Ultrasound, Mumbai, India). The photosonation system composed of ultrasonic processor and ultraviolet lamps (Cole Parmer, Pen-Ray UV lamps– 254 nm). They are equipped with 2 ultraviolet lamps in parallel (4.4 mW cm⁻²each) for photocatalytic degradation. The ultrasound probe was immersed into the solution at a depth of approximately 3 cm within a 250 mL Ponceau S sample in 500 mL glass reactor with cooling jacket. The experiments were carried out using the amplitude level of 90 %. The power level (Watts) was measured 95 W by using Powmet-230 Power

Meter. The reaction temperature of 20 ± 2 °C was maintained by circulating water. The absorbance of the sample was measured by means of UV-VIS spectrophotometer (Systronics model-2203) at the λ_{\max} 520 nm. The absorption was converted into concentration through the standard curve of Ponceau S. The pH of solution was maintained by using 0.1 M HCl and 0.1 M NaOH. Stock dye solutions were prepared by dissolving 1 g of Ponceau S in 1 L of double distilled water.

Table 1. Characteristics of Ponceau S.

IUPAC name	Structure	$\lambda_{\max}(\text{nm})$	Molecular weight
tetrasodium;(4E)-3-oxo-4-[[2-sulfonato-4-[(4-sulfonatophenyl) diazenyl]phenyl]hydrazinylidene]naphthalene-2,7-disulfonate		520	672.63 mol ⁻¹

2.2. Synthesis of Fe-doped ZnO nanoparticles.

The aqueous solutions of $\text{ZnSO}_4 \cdot 7\text{H}_2\text{O}$ and $\text{FeSO}_4 \cdot 7\text{H}_2\text{O}$ were prepared in distilled water in the desired ratio (Fe/Zn being 5 % molar ratio). The mixed solutions were sonicated for 2 h using probe sonicator. After sonication the mixed solutions were continuously stirred for 30 min. In order to avoid agglomeration in acidic and neutral condition and to obtain one-phase Fe-doped ZnO, an appropriate amount of NaOH in an aqueous solution was added to the solution until a pH of 12 was reached. The resulting solution was again stirred for 30 min, and then it was allowed to stand at room temperature for 18 h. Next, the solution was centrifuged and washed several times with distilled water and ethanol in order to remove residual and unwanted impurities. The final product was dried in a vacuum oven at 200 °C for 1 h yielding the brown Fe-doped ZnO powder [23].

3. Results and Discussion

3.1. SEM and EDX analysis

Scanning electron micrographs (SEM) was recorded to obtain the shape and diameter of particles (Fig. 1a). The results showed that spherical particles were well distributed and the average particle size was less than 71 nm. The EDX analysis Fig. 1(b) shows that nano Fe-doped ZnO contains Fe K (18.73 %), Zn K (14.81 %) and O K (66.47 %).

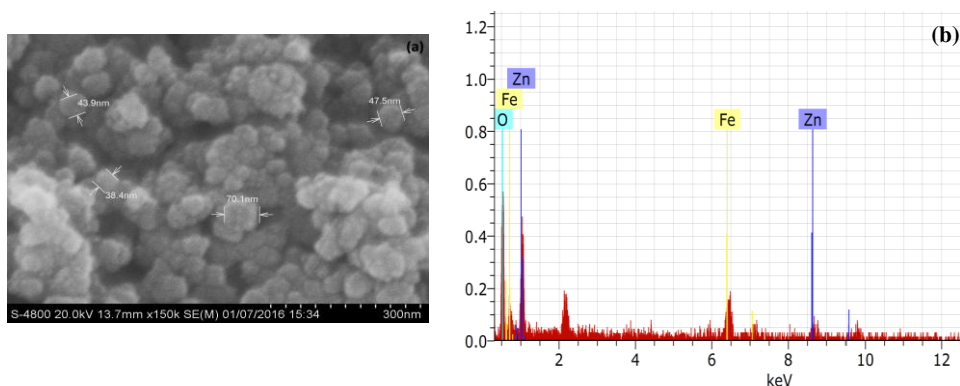


Fig. 1. SEM image (a) and EDX (b) of Fe-doped ZnO nano catalyst.

3.2. X-ray diffraction analysis

XRD patterns of undoped and Fe doped ZnO nanoparticles shown in Fig. 1 were determined by X-ray diffractometer with $\text{CuK}\alpha$ radiations ($\lambda = 1.5416\text{\AA}$) in the range of 20° to 80° at room temperature. The sharp intense peak obtained in all the samples at $2\theta \approx 30.80, 34.22, 35.38, 46.70, 54.88, 62.02, 64.13, 66.20, 66.84, 72.24$ and 74.76 corresponds to the lattice plane (100), (002), (101), (102), (110), (103), (200), (112), (201), (004) and (202) respectively confirms that the prepared samples are good crystalline in nature with wurtzite hexagonal structure and are agree with the JCPDS data (01-075-1533). The results suggest that doping ZnO with Fe at concentrations up to certain level does not significantly alter the wurtzite ZnO nanoparticles. It is observed that doping of Fe, the intensity of main diffraction peaks slightly shifted towards lower angle, which suggest that Fe doping decreased the crystalline quality and crystallite size of ZnO nanoparticles [24]. The crystallite size (D) was calculated from line broadening of the major XRD peak (101) using the Scherrer's formula [25].

$$D = \frac{K\lambda}{\beta \cos\theta} \quad (1)$$

Where, K is the shape factor, which is a constant taken as 0.9, λ is the wavelength of the X-ray radiation ($\lambda = 1.5416\text{\AA}$), β is the full-width at half-maximum (FWHM) in radians, θ is the Bragg's angle in degree. The crystallite size of the undoped and Fe doped ZnO samples obtained from equation (1) are 26.90 and 23.48 nm respectively.

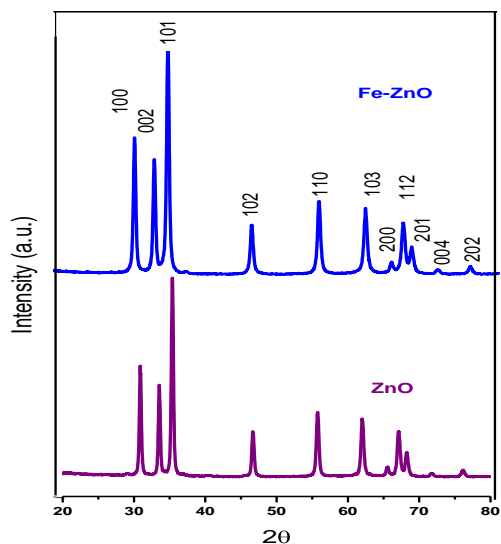


Fig. 2. XRD diagram of undoped and Fe doped ZnO nano catalyst.

3.3. *Effect of pH*

Generally, the pH of solution is practically important in wastewater treatment and is a key factor affecting on the ultrasonic, sonocatalytic, photocatalytic and sonophotocatalytic degradation process of organic compounds [18]. Since it could change the surface charge of the catalyst, thus the degradation performance of organic molecules on the catalyst surface could be changed. Moreover, the molecular structure of the organic dye can be influenced when pH solution changes and becomes easier to degrade. To study the effect of pH of the solution on the degradation of the Ponceau S, the experiments were carried out in a range of pH 2 to 12. The initial dye concentration was 40 mg/L for 1 g/L of ZnO and Fe doped ZnO nano catalysts which were kept constant. The graph of percent degradation verses pH shows higher degradation percentage in acidic media (pH=4). It has been observed that a pH increase from 2 to 4, percent degradation increases and then decrease up to pH 12 for ultrasonic, sonocatalytic, photocatalytic and sonophotocatalytic degradation respectively. This can be explained on the basis of zero point charge (zpc). The pH_{zpc} is 8.1 for Fe-doped ZnO. Therefore, the surface of Fe-doped ZnO and ZnO is positively charged below the zpc and negatively charged above the zpc. From the experiments, it was found that the optimum pH solution to degrade Ponceau S, this is due to the electrostatic attraction between the dye molecules and positive Fe-doped ZnO surface is very high. Hence, more molecules are degrading on the surface of the sonocatalyst, photocatalyst and sonophotocatalyst. The decrease in ultrasonic, sonocatalytic, photocatalytic and sonophotocatalytic degradation at high alkaline pH is due to the electrostatic repulsion between the negatively charged molecules. Moreover, due to the presence of high amounts of $\cdot\text{OH}$ radicals, the radical-radical reactions take

place at higher pH values. Satheesh *et al.* reported this deactivation phenomenon at higher pH values [26].

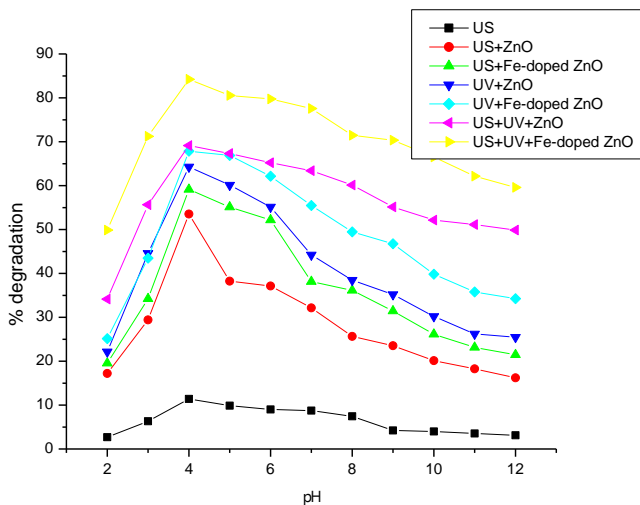


Fig. 3. Effect of pH on ultrasonic, sonocatalytic, photocatalytic and sonophotocatalytic degradation of Ponceau S after 120 min.

3.4. Degradation study

3.4.1. Effect of sonocatalyst, photocatalyst and sonophotocatalyst dosage.

To investigate the effect of catalyst loading on the degradation rate of Ponceau S dye experiments were conducted for catalyst loadings as 0.5, and 1.0 g/L, at initial dye concentration of 40 mg/L and at pH 4. The obtained results have been given in Fig. 4(a-c). It can be seen from the figures that the extent of degradation increased significantly with an increase in the catalyst dosage up to 0.5 and 1.0 g/L. For undoped sonocatalyst, photocatalyst and sonophotocatalyst samples the percentage degradation observed to be 17 %, 27 % and 37 % were achieved with 0.5 g/L and maximum extent of degradation was observed to be 44 %, 51 % and 92 % at the catalyst dosage of 1.0 g/L. For doped sonocatalyst, photocatalyst and sonophotocatalyst samples the percentage degradation observed to be 27 %, 32 % and 55 % at the catalyst dosage of 0.5 g/L and maximum extent of degradation was observed as 55 %, 65 % and 96 % at the catalyst dosage of 1.0 g/L. It was observed that there was major difference in the degradation efficiencies for 0.5 and 1.0 g/L catalyst loadings. The percentage degradation was observed to be higher for Fe-doped ZnO than undoped ZnO for 0.5 g/L and 1.0 g/L catalyst dose that is dose of catalyst increases percentage degradation for all the systems studied. The adequate loading of the catalyst can increase the generation rate of electron/hole pairs for

enhancing the degradation of pollutants. At higher loadings, the catalysts may block the light irradiation, and restrain the effective usage of light for photo excitation [27-29]. Thus, the results indicate that increase in catalyst loading increase the percentage degradation. The dye degradation was observed to attain the equilibrium after 90 min. For further study it was considered as the optimum time.

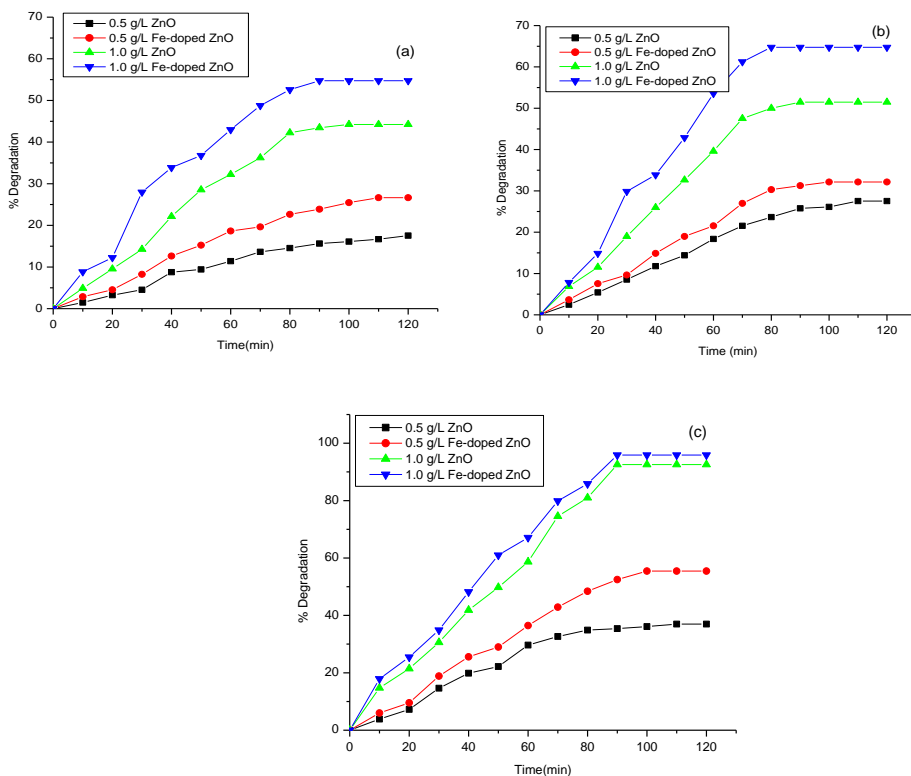


Fig. 4. Effect of catalyst loading on percentage degradation (a) Sonocatalyst, (b) Photocatalyst, (c) Sonophotocatalyst.

3.4.2. *Effect of initial dye concentration*

Fig. 5 illustrates the variation in the relative concentration, C/C_0 with irradiation time for two initial concentrations of Ponceau S as 20 and 40 mg/L. The experiments have been conducted at pH 4 and catalyst dose was 1.0 g/L. It can be seen that higher the initial concentration, the lower is the observed degradation. This negative effect may be because of the following reasons (i) when the Ponceau S concentration increases the amount of degradation on the catalyst surface increases. The increase in Ponceau S concentration will decrease the path length of photons entering the solution. In addition to this, at a high Ponceau S concentration, a significant amount of UV light may be absorbed by the dye molecules rather than by the catalyst particles and that reduces the efficiency of the

catalytic reaction, (ii) the percentage degradation is dependent on the probability of $\bullet\text{OH}$ radicals formation on the catalyst surface and the probability of $\bullet\text{OH}$ radicals reacting with dye molecules. But at high dye concentrations the generation of $\bullet\text{OH}$ radicals on the surface of catalyst are likely to be reduced since active sites are covered by ions. Thus, the limitation of surface sites for the reaction may control the final extent of degradation, (iii) the reduction in the degradation of Ponceau S can also be attributed to the filter effect caused by absorption of photon energy by the Ponceau S molecules, (iv) the relatively longer chain of Ponceau S cannot completely enter the electron-hole, and thus reduces the degradation rate. The results clearly indicate that the sonophotocatalytic degradation process is promising at low concentrations of the pollutant. This is also true for heterogeneous catalytic systems where the reaction occurs at the interface between two phases [30,31,33].

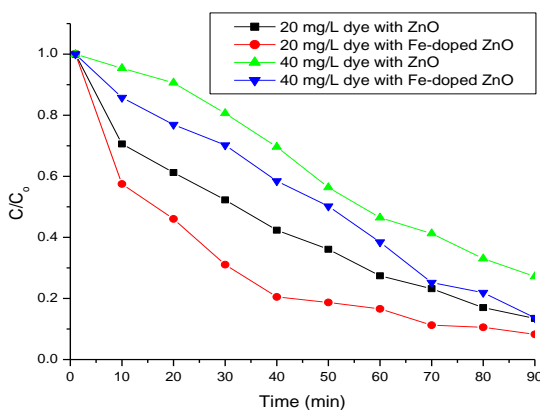


Fig. 5. Effect of initial dye concentration of Ponceau S using sonophotocatalyst.

3.4.3. Comparison for sonolysis, sonocatalysis, photocatalysis, and sonophotocatalysis degradation

The results indicate that sonocatalytic, photocatalytic and sonophotocatalytic activity of Fe-doped ZnO was higher than those of the direct sonocatalytic, photocatalytic and sonophotocatalytic by undoped ZnO nano catalyst. It was observed that the degradation rate is higher for doped catalyst in all systems like sonocatalyst, photocatalyst and sonophotocatalyst as compared to undoped ZnO. Such combination leads to additive effects and is effective than sonolysis, sonocatalysis and photocatalysis only. Therefore, sonophotocatalytic degradation of Ponceau S was investigated under ultrasonic and UV light irradiation. All degradation processes were carried out under the same conditions which are described for sonolysis, sonocatalysis, photocatalysis and sonophotocatalysis. According to the electric field theory, the fragmentation of microbubbles induced by ultrasound is accompanied by the formation of places of high density of negative charge

that can produce intense electric fields when those bubbles come near to the locally charged doped and undoped ZnO nano catalyst [32]. The strong electric fields produced in this way can induce local discharges that can promote many chemical and physical processes that can increase the degradation rate of Ponceau S on the surface of ZnO and Fe-doped ZnO nano catalysts.

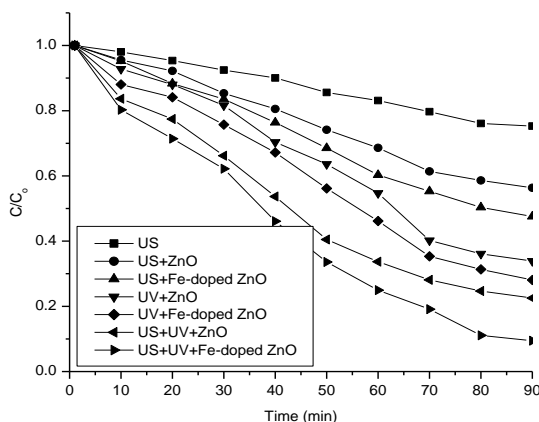


Fig. 6. Comparison of sonolysis, sonocatalysis, photocatalysis and sonophotocatalysis processes for degradation of Ponceau S at US power 150 W.

3.4.4. *Effect of H₂O₂ on sonocatalytic degradation*

The experiments have been conducted to investigate Ponceau S degradation in different systems at a pH 4, 1 g/L ZnO or Fe-doped ZnO and 75 mg/L of (20 V/V) H₂O₂ (Fig. 7). It was observed that 18, 33, 49, 54, 63 and 69 % of Ponceau S dye were degraded using US, US+H₂O₂, US+ZnO, US+ZnO+H₂O₂, US+Fe-doped ZnO and US+Fe-doped ZnO+H₂O₂ in 90 min, respectively (Fig. 7). It can be observed that Ponceau S dye degradation efficiency in the US/Fe-doped ZnO/H₂O₂ process was higher than the sonocatalytic process, which was mainly ascribed to the promotion of ultrasound on Fe-doped ZnO catalyzed degradation of H₂O₂ to form more active free radicals (\bullet OH). The percentage of degradation was very low (18 %) by sonication alone, since Ponceau S is a non-volatile compound and the place of degradation would be mostly at the exterior of the cavitation bubbles. One of the more popular AOP methods for wastewater degradation is oxidation with H₂O₂ which, due to its stability in pure form, needs to be activated [33]. This would result in the faster degradation of H₂O₂ to generate \bullet OH radicals [34].

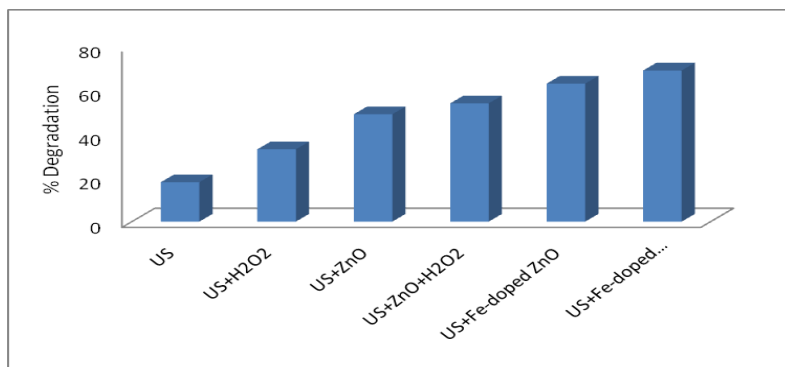


Fig. 7. Effect of H₂O₂ on sonocatalyst system.

3.4.5. Effect of H₂O₂ on photocatalytic degradation

One possible way to enhance degradation of the compound would be to increase the concentration of •OH radicals, because these species are widely considered to be promoters of photocatalytic degradation [35]. •OH radicals are generated from H₂O₂ under UV irradiation. The percent degradation increases with H₂O₂ addition. At a constant UV intensity, as amount of H₂O₂ increases, more •OH radicals are produced which results in high degradation rate [36]. The effect of H₂O₂ on photocatalytic degradation of Ponceau S was studied with an initial dye concentration of 40 mg/L, pH 4 and catalyst dose 1 g/L (Fig. 8). Under UV irradiation 14 % degradation of Ponceau S was achieved within 90 min. However, the degradation decreased to 8 % through the UV+H₂O₂. This may be due to the fact that H₂O₂ scavenges the photo-generated oxidizing species (i.e., valence band holes and hydroxyl radicals) that are responsible for oxidation of dye molecule (Eqs. (2) and (3)) [37].



The degradation of Ponceau S was 14% in UV, 8 % in UV+H₂O₂, 51 % UV+ZnO, 56 % US+ZnO+H₂O₂, 61 % US+Fe-doped ZnO, 68 % US+Fe-doped ZnO+ H₂O₂. This is probably due to the more formation of hydroxyl radicals by the photochemical splitting of water. This clearly indicates that both catalyst and irradiation are necessary for the destruction of this dye [35].

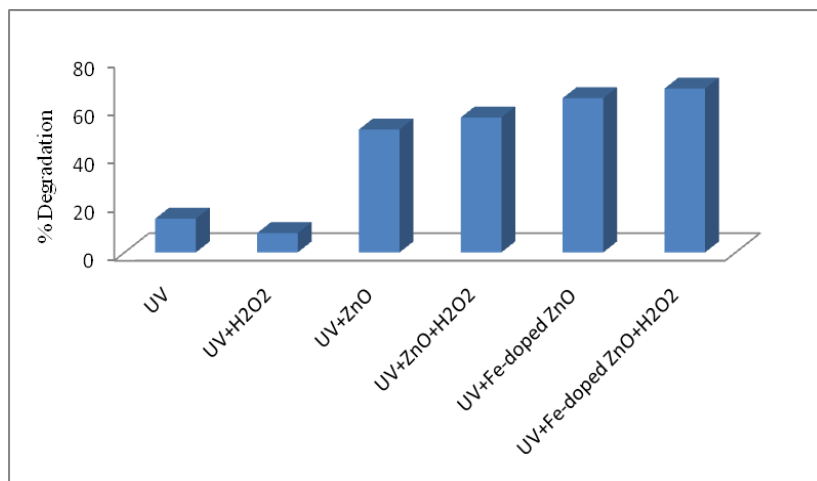


Fig. 8. Effect of H₂O₂ on photocatalyst system.

3.4.6. *Effect of H₂O₂ on sonophotocatalytic systems*

H₂O₂ assisted sonophotocatalytic oxidation was carried out for 40 mg/L Ponceau S dye concentration. The addition of H₂O₂ with catalysis increases the efficiency of dye degradation. The purpose of using H₂O₂ is to provide an additional source of hydroxyl radicals in the system as it is known that both cavitation conditions and UV light results in dissociation of H₂O₂ to give hydroxyl radicals [38]. However, the dye degradation yield was 33 % in the US/UV/H₂O₂ process, while it was 44 % in the US/UV process. The reason is that a greater dosage of H₂O₂ produces more hydroxyl radicals that result in a higher degradation at a constant UV intensity. However, in the excess of H₂O₂, hydroxyl radicals are consumed to form hydroperoxyl radical that have lower oxidation capability (Eqs. (2) and (3)) [36]. The dye degradation was 91 % for US+UV+ZnO+H₂O₂ and 98 % US+UV+Fe-doped ZnO+H₂O₂ combination, while it was 69 % in US+UV+ZnO and 79 % US+UV+Fe-doped ZnO (Fig. 9). A greater extent of degradation was observed for doped sonophotocatalysis (US+UV+Fe-doped ZnO+H₂O₂) compared with the individual doped and undoped processes.

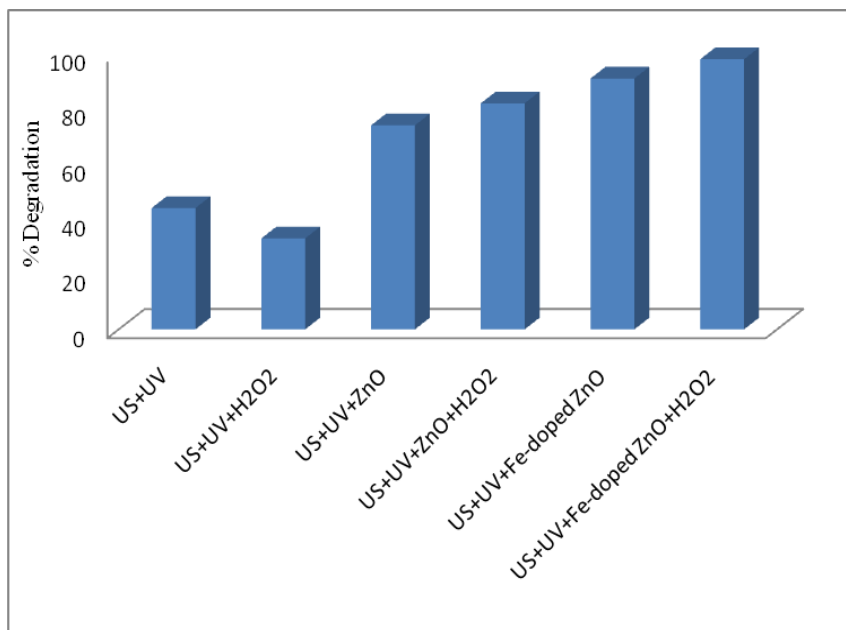


Fig. 9. Effect of H₂O₂ on sonophotocatalyst system.

3.4.7. Kinetics of the degradation

Kinetics of ultrasonic, sonocatalytic, photocatalytic and sonophotocatalytic degradation of Ponceau S has been investigated. The pseudo-first order reaction kinetics can be represented by the following equation.

$$-\ln(C_0/C)=kt \quad (4)$$

Where C is the final concentration (mg/L) of Ponceau S after irradiation, C₀ is the initial concentration (mg/L) of Ponceau S, t is the irradiation time (min) and k is the apparent reaction rate constant (min⁻¹). The kinetic studies have been performed for the sonochemically prepared catalysts with the optimum doping content for iron and also comparison has been done with the sonolysis, sonocatalysis, photocatalysis and sonophotocatalysis process gives the first-order reaction kinetics for degradation of Ponceau S. The regression coefficient R² obtained for first order reaction at different experimental conditions which ranges from 0.96 to 0.99, confirming that degradation of Ponceau S under different experimental conditions i.e., doped and undoped sonolysis, sonocatalysis, photocatalysis and sonophotocatalysis follows the first order reaction. Very slow degradation rate was observed in the presence of only US without doped, undoped ZnO. The slightly increase in degradation rate was observed in ultrasound in presence of doped, undoped ZnO, while the degradation occurred at higher rate under sonophotocatalysis. The results have clearly indicated that, the better efficacy of the doped sonophotocatalyst as compared to the undoped sonophotocatalyst catalyst.

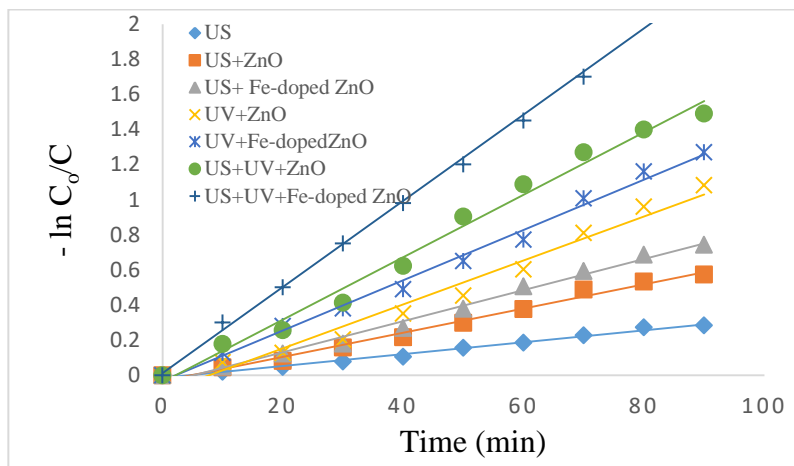


Fig. 10. First order kinetics plot of Ponceau S degradation in presence of doped and undoped ZnO nan catalyst under sonolysis, sonocatalysis, photocatalysis and sonophotocatalysis.

The efficacy of photocatalytic degradation under optimized conditions is shown in Fig. 11. This shows clearly the effectiveness of decolorization and degradation capacity of Fe-doped ZnO after 90 min under sonophotocatalytic conditions.

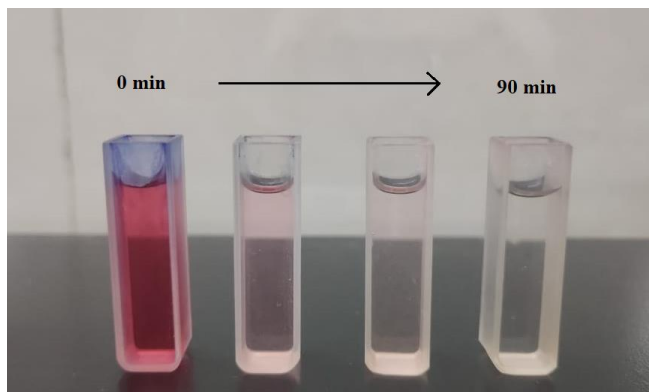


Fig. 11. Degradation capacity of Fe-doped ZnO.

4. Conclusion

Fe-doped ZnO nano catalyst was synthesized by co-precipitation method. A systematic study of the structural morphology and sonocatalytic, photocatalytic and sonophotocatalytic activity under UV irradiation have been performed using various techniques. The effect of pH on the sonocatalytic, photocatalytic and sonophotocatalytic activity was investigated. The results indicated that an acidic medium (pH 4) is appropriate for the degradation of Ponceau S dye and the degradation of Ponceau S increased with the increase of catalyst dose, while the degradation percentage decreased

with the increase of initial concentration of Ponceau S. The Effect of H₂O₂ is an additive effect for degradation of Ponceau S, the results indicate that addition of H₂O₂ in presence of sonophotocatalyst increased the degradation. The Fe-doped ZnO nano catalyst is suitable for degradation of Ponceau S under sonophotocatalyst than sonocatalyst and photocatalyst. The ultrasonic, sonocatalytic, photocatalytic and sonophotocatalytic degradations followed first order kinetics and overall, it can be said that Ponceau S was effectively degraded 98 % within 90 min in presence Fe-doped ZnO nano catalyst under sonophotocatalytic degradation.

Acknowledgements

The authors are very much thankful to Central Instrumentation Centre, University Institute of Chemical Technology, NMU Jalgaon for SEM, EDX and XRD analysis. The authors also thankful to Principal, Kisan Arts, Commerce and Science College, Parola, Dist. Jalgaon (M.S.) for providing necessary laboratory facilities.

References

1. M. Ying-Shih, S. Chi-Fanga, and L. Jih-Gaw, J. Hazardous Mater. **178**, 320 (2010). <https://doi.org/10.1016/j.jhazmat.2010.01.081>
2. R. Zouaghi, B. David, J. Suptil, K. Djebbar, A. Boutiti, and S. Guittoneau, Ultrason. Sonochem. **18**, 1107 (2011). <https://doi.org/10.1016/j.ultsonch.2011.03.008>
3. R.A. Torres, F. Abdelmalek, E. Combet, C. Petrier, and C. A. Pulgarin, J. Hazard. Mater. **146**, 546 (2007). <https://doi.org/10.1016/j.jhazmat.2007.04.056>
4. R. Farouq, J. Chin. Chem. Soc. **65**, 1333 (2018). <https://doi.org/10.1002/jccs.201800029>
5. S. Malato, J. Blanco, D. C. Alarcon, M. I. Maldonado, P. Fernandez-Ibanez, and W. Gernjak, Catal. Today **122**, 137 (2007). <https://doi.org/10.1016/j.cattod.2007.01.034>
6. S. G. Shelar, V. K. Mahajan, S. P. Patil, and G. H. Sonawane, J. Mater. Environ. Sci. **10**, 431 (2019).
7. H. Lachheb, E. Puzenat, and A. Houas, Appl. Catal. B: Environ. **39**, 75 (2002). [https://doi.org/10.1016/S0926-3373\(02\)00078-4](https://doi.org/10.1016/S0926-3373(02)00078-4)
8. R. A. Torres, J. I. Nieto, and E. Combet, Appl. Catal. B: Environ. **80**, 168 (2008). <https://doi.org/10.1016/j.apcatb.2007.11.013>
9. P. Kanthale, M. Ashokkumar, and F. Grieser, Ultrason. Sonochem. **15**, 143 (2008). <https://doi.org/10.1016/j.apcatb.2007.11.013>
10. Y. Zhai, Y. Li, J. Wang, J. Wang, L. Yin, Y. Kong, G. Han, and P. Fan, J. Mol. Catal. A: Chem. **366**, 282 (2013). <https://doi.org/10.1016/j.molcata.2012.10.006>
11. H.V. Vasei, and S. Masoudpanah, J. Mater. Res. Technol. **11**, 112 (2021). <https://doi.org/10.1016/j.physb.2021.413130>
12. T. Abdel-Baset and M. Belhaj, Phys. B **616**, ID 413130 (2021). <https://doi.org/10.1016/j.physb.2021.413130>
13. N. Q. Yang, J. Li, Y. N. Wang, and J. Ma, Mater. Sci. Semicond. Process **131**, ID 105835 (2021). <https://doi.org/10.1016/j.mssp.2021.105835>
14. R. T. Sapkal, S. S. Shinde, T. R. Waghmode, S. P. Govindwar, K. Y. Rajpure, and C. H. Bhosale, J. Photochem. Photobiol. B: Biology **110**, 15 (2012). <https://doi.org/10.1016/j.jphotobiol.2012.02.004>
15. L. Zhang, H. Cheng, R. Zong, and Y. Zhu, J. Phys. Chem. C **113**, 2368 (2009). <https://doi.org/10.1021/jp807778r>

16. N. V. Kaneva, D. T. Dimitrov, and C. D. Dushkin, *Appl. Surf. Sci.* **257**, 8113 (2011).
<https://doi.org/10.1016/j.apsusc.2011.04.119>
17. R. S. Ajimsha, A. K. Das, B. N. Singh, P. Misra, and L. M. Kukreja, *Phys. E* **42**, 1838 (2010).
<https://doi.org/10.1016/j.apsusc.2016.06.114>
18. M. Khatamian, A. A. Khandar, B. Divband, M. Haghghi, and S. Ebrahimiasl, *J. Mol. Catal. A: Chem.* **365**, 120 (2012). <https://doi.org/10.1016/j.molcata.2012.08.018>
19. H. Zhang, R. Zong, and Y. Zho, *J. Phys. Chem. C* **113**, 4605 (2009)
<https://doi.org/10.1021/jp810748u>
20. R. Saleh, and N. F. Djaja, *Superlattices and Microstructures* **74**, 217 (2014).
<https://doi.org/10.1016/j.spmi.2014.06.013>
21. P. K. Labhane, V. R. Huse, L. B. Patle, A. L. Chaudhari and G. H. Sonawane, *J. Mater. Sci. Chem. Engg.* **3**, 39 (2015). <https://doi.org/10.4236/MSCE.2015.37005>
22. B. Tural, Ş. BetülSopacı, NecatiÖzkan, A. S. Demir, and M. Volkan, *J. Phys. Chem. Solids* **72**, 968 (2011). <https://doi.org/10.1016/j.jpcs.2011.05.010>
23. A. Mancuso, O. Sacco, S. Mottola, S. Pragliola, A. Moretta, V. Vaiano, and I. De Marco, *Inorganica Chimica Acta* **549**, ID 121407 (2023). <https://doi.org/10.1016/j.ica.2023.121407>
24. H. Sutanto, I. Alkian, M. Mukholit, A.A. Nugraha, E. Hidayanto, I. Marhaendrajaya, and P. Priyono, *Mater. Res. Expr.* **8**, 116402 (2021). <https://doi.org/10.1088/2053-1591/ac33fe>
25. E.M. Modan, and A.G. Plăiaşu, *The Annals of “Dunarea de Jos” University of Galati, Fascicle IX, Metall. Mater. Sci.* **43**, 53 (2020). <https://doi.org/10.35219/mms.2020.1.08>
26. R. Satheesh, K. Vignesh, A. Suganthi, and M. Rajarajan, *J. Environ. Chem. Eng.* **2**, 1956 (2014). <https://doi.org/10.1016/j.jece.2014.08.016>
27. S. S. Ashraf, M. A. Rauf, and S. Alhadrami, *Dyes Pigm.* **69**, 74 (2006).
<https://doi.org/10.1016/j.dyepig.2005.02.009>
28. H. Wang, J. Niu, X. Long, and Y. He, *Ultrason. Sonochem.* **15**, 386 (2008).
<https://doi.org/10.1016/j.ultsonch.2007.09.011>
29. F. Hossain, Md. A. Rahman, and Md. M. Hossain, *Dhaka Univ. J. Sci.* **69**, 218 (2022).
<https://doi.org/10.3329/dujs.v69i3.60033>
30. F. I. Kiriakidou, D. I. Kondarides, and X. E. Verykios, *Catal. Today* **54**, 119 (1999).
[https://doi.org/10.1016/S0920-5861\(99\)00174-1](https://doi.org/10.1016/S0920-5861(99)00174-1)
31. M. Asilturk, F. Sayilkan, and E. Arpac, *J. Photochem. Photobiol. A: Chem.* **203**, 64 (2009).
<https://doi.org/10.1016/j.jphotochem.2008.12.021>
32. K. Nomiya, S. Matsuoka, T. Hasegawa, and Y. Nemoto, *J. Mol. Catal. A: Chem.* **156**, 143 (2000). [https://doi.org/10.1016/S1381-1169\(99\)00283-6](https://doi.org/10.1016/S1381-1169(99)00283-6)
33. Z. Eren, and N. H. Ince, *J. Hazardous Mater.* **177**, 1019 (2010).
<https://doi.org/10.1016/j.jhazmat.2010.01.021>
34. Y. L. Song and J. T. Li, *Ultrason. Sonochem.* **16**, 440 (2009).
<https://doi.org/10.1016/j.ultsonch.2008.12.011>
35. Y. Liu, L. Hua, and S. Li, *Desalination* **258**, 48 (2010).
<https://doi.org/10.1016/j.desal.2010.03.050>
36. M. W. Chang, C. C. Chung, J. M. Chern, and T. S. Chen, *Chem. Eng. Sci.* **65**, 135 (2010).
<https://doi.org/10.1016/j.ces.2009.01.056>
37. F. Ahmedchekkat, M. S. Medjram, M. Chiha, and A. M. A. Al-bsoul, *Chem. Eng. J.* **178**, 244 (2011). <https://doi.org/10.1016/j.cej.2011.10.061>
38. K. P. Mishra, R. Parag, and P. R. Gogate, *Ultrason. Sonochem.* **18**, 739 (2011).
<https://doi.org/10.1016/j.ultsonch.2010.11.004>